IEEE Access
Multidisciplinary ⋮ Rapid Review ⋮ Open Access Journal

Received 8 September 2023, accepted 31 October 2023, date of publication 6 November 2023, date of current version 9 November 2023.

Digital Object Identifier 10.1109/ACCESS.2023.3330495

RESEARCH ARTICLE

Parameter Identification of Permanent Magnet Synchronous Motor Based on CGCRAO Algorithm

HONGJI LI AND XIANZHONG JIAN
School of Optoelectronic Information and Computer Engineering, University of Shanghai for Science and Technology, Shanghai 200093, China
Corresponding author: Xianzhong Jian (jianxz@usst.edu.cn)

This work was supported in part by the National Natural Science Foundation of China under Grant 11774017.

ABSTRACT In response to the challenge of easily falling into local optima and slow identification speed in the parameter identification of permanent magnet synchronous motors (PMSMs), this paper proposes a novel algorithm called the Chaotic Gaussian-Cauchy RAO (CGCRAO) algorithm, which leverages chaotic initialization and a hybrid variation strategy. The algorithm uses Tent chaotic mapping for population initialization to improve population diversity. At the same time, by combining the Gaussian and Cauchy distribution characteristics and the three-stage operation idea, the optimal individual variation strategy is autonomously selected in real-time to improve the RAO-1 algorithm. This paper validates the effectiveness of the algorithm improvement and the correctness of the three-stage operation idea using eight benchmark test functions. Furthermore, This paper conducted comparative experiments on parameter identification of five algorithms under different operating conditions through simulation and experiments. The results indicate that the proposed CGCRAO algorithm enables fast and accurate identification of PMSM parameters.

INDEX TERMS CGCRAO algorithm, permanent magnet synchronous motors (PMSMs), three-stage running idea, chaos initialization, Gaussian-Cauchy hybrid variation.

I. INTRODUCTION

The permanent magnet synchronous motor (PMSM) is a type of motor that has outstanding advantages such as small size, simple structure, high power density, and stable performance. It has been widely used in high-performance fields such as aerospace [1], industrial production [2], and transportation [3], [4]. To achieve efficient control of PMSMs in these fields, scholars have designed many advanced controllers, such as field-oriented control (FOC) [5] and direct torque control (DTC) [6]. The accurate model and parameters of the PMSM are crucial for the performance release of these controls and the design of fault diagnosis systems [7].

In PMSM DTC [5], electromagnetic torque and magnetic flux are critical control variables. However, inter-turn short circuits can cause sudden changes in the dq-axis inductance and stator winding resistance. In contrast, demagnetization of the rotor permanent magnet can cause a decrease in magnetic flux amplitude. These factors seriously affect the control effect of DTC. For PMSM FOC [8], the PID parameters in the current control loop are closely related to the inherent parameters of the motor, such as the stator resistance, dq-axis inductance, and rotor magnetic flux. However, the motor parameters are easily affected by temperature changes, skin effect, and magnetic saturation, which can lead to poor control performance of the PID controller and thus affect the motor's operating performance. Therefore, to achieve high dynamic response and high-precision control, accurate motor parameters are needed, and fast and effective parameter identification methods are required to improve the control performance of the entire servo system [9].

The search for more accurate and effective methods of identifying the parameters of PMSMs has become a widely studied topic among researchers. Currently, these research efforts can be divided into two categories: traditional identification methods and identification methods based on artificial intelligence optimization algorithms. Traditional identification methods include Recursive Least Squares (RLS) [10], [11], [12], Model Reference Adaptive

The associate editor coordinating the review of this manuscript and approving it for publication was Diego Oliva.

Systems (MRAS) [13], [14], [15], [16], and Extended Kalman Filters (EKF) [17], [18], [19]. The RLS method linearizes the mathematical model of the motor, which is easy to implement but requires a large amount of computation and data storage space. Additionally, the RLS method requires the derivative of the objective function concerning the motor parameters. However, external noise and fluctuations in motor speed can affect the differentiation results, leading to poor robustness of the RLS method [10], [11]. To address this issue, a PMSM parameter identification method based on recursive least squares with a forgetting factor and a weighting factor was proposed in [12]. However, due to the different algorithm parameter selections under different motor operating conditions, it is difficult to simultaneously achieve good identification accuracy and algorithm tracking performance. The MRAS method can identify the stator resistance and rotor magnetic flux well, but the design of the adaptive rule is complex and difficult, resulting in reduced accuracy [13], [14]. In [16], some parameters with small variations were taken as fixed values to identify other motor parameters. Still, the varying parameters themselves change with the motor operation, leading to large identification errors. The EKF method overcomes the problem that the MRAS method is only applicable to linear systems and is sensitive to external noise but requires a large amount of matrix calculation at each step, resulting in a huge computational load [17]. Additionally, the EKF method requires accurate pre-processing of the motor mathematical model, which is also complex when identifying multiple parameters [19].

The PMSM has nonlinear and time-varying characteristics. Traditional parameter identification methods cannot achieve a good balance in factors such as convergence, complexity, and convergence accuracy [20]. In recent years, artificial intelligence optimization algorithms have achieved good results in solving many optimization problems due to their low requirements on the objective function and high efficiency, and have begun to be applied in the PMSM field. For example, [21] applied neural network algorithms (NNA) to high-speed PMSM parameter identification. Although NNA can obtain more accurate results in parameter identification, it usually requires a large number of data samples for training and timely information adjustment. At the same time, users cannot intervene in the operation, making it difficult to find the causes of erroneous results. In addition, [22] used a particle swarm optimization algorithm to identify PMSM parameters, which transforms the system parameter identification problem into a multimodal dynamic optimization problem. This algorithm has high identification accuracy for stator resistance, but low accuracy for magnetic flux and dq-axis inductance. Later, researchers improved the algorithm to introduce Cauchy variation into the particle swarm algorithm, using the Cauchy perturbation strategy to enhance the global exploration ability of the particle swarm algorithm and thereby improve the parameter identification accuracy [23], but further improvement is still needed. Meanwhile, [24] proposed a dynamic self-learning particle swarm optimization algorithm based on the traditional particle swarm method, which enhanced the population's global search ability and escaped local optima. Reference [25] introduced a nonlinear convergence strategy based on the original GWO algorithm to improve the algorithm's global search ability and to some extent, improve the convergence accuracy, but the convergence speed still needs to be improved. In addition, [26] proposed an improved differential evolution algorithm (DE) that introduced cloning selection and receptor editing mechanisms to improve the algorithm's population diversity and global search ability. However, this algorithm is only applicable to non-convex extreme PMSMs, and parameter identification of convex extreme PMSMs still needs further research. References [27], [28], and [29] combined the differential evolution algorithm with the particle swarm optimization algorithm and applied them to parameter identification under different backgrounds. This hybrid algorithm avoids the shortcomings of the two algorithms and has good parameter identification accuracy, but the hybrid formula is complex, with many parameters, and the algorithm time complexity is high. Reference [30] proposed a hybrid variation adaptive differential evolution algorithm to solve the problem of scaling factors and crossover roads difficult to determine in traditional differential evolution algorithms. This algorithm has better application in the PMSM parameter identification field and can effectively reduce identification errors. However, the algorithm itself is complex, using random numbers for variation, and its global exploration ability and local mining ability still need to be further improved. RAO-1 is another implicit optimization algorithm proposed by Ravipudi Venkata Rao in 2020 after the JAYA algorithm [31]. The core formula of this algorithm is simple, with few algorithm parameters, and easy to embed in embedded systems. However, it has the disadvantages of poor population diversity and the inability to accurately search for optimization in the later stages of iteration.

To address the above-mentioned issue, this paper proposes a hybrid variation-based chaotic RAO algorithm for PMSM parameter identification. In the algorithm initialization stage, Tent chaotic mapping is first used to enhance the diversity of the population. Subsequently, the algorithm is combined with the Gauss-Cauchy variation strategy based on the three-stage idea proposed in this paper, which effectively improves the local exploitation and global exploration abilities of the algorithm. Eight standard test functions are used for verification. Finally, a dual-loop PMSM simulation model and hardware experimental platform based on vector control and feedforward decoupling control were constructed. The superiority of the CGCRAO algorithm was validated through parameter identification and comparison with the identification results of four other algorithms.

The main contributions of this paper are as follows: Firstly, an improved RAO-1 algorithm, CGCRAO, is proposed for

PMSM parameter identification. The algorithm utilizes Tent chaotic mapping to initialize the population and incorporates the Gaussian-Cauchy function to guide the variation process. Secondly, a three-stage idea is introduced to guide the variation process based on the changing curve of the fitness function during the algorithm iterations. Thirdly, the effectiveness of the CGCRAO algorithm improvement and the correctness of the three-stage idea is verified by using eight standard test functions. The simulation model and hardware experimental platform for PMSM were established. Comparative experiments were conducted for parameter identification using five different algorithms, further validating the feasibility and superiority of the CGCRAO algorithm.

The structure of this paper is as follows: Section II introduces the mathematical model of PMSM. Section III elaborates on the principles of the CGCRAO algorithm, focusing on the core formulas, initialization strategies, and variation strategies of the basic version. By validating with eight benchmark test functions, the improved performance of the CGCRAO algorithm is demonstrated. Section IV introduces the PMSM parameter identification model. Sections V and VI present the comparative results of algorithm identification in both the simulation environment and the hardware experimental environment. Finally, Section VII provides a summary of the entire paper.

II. MATHEMATICAL MODEL OF PMSM

PMSM is a complex system that exhibits strong coupling, nonlinearity, and time variation. To facilitate analysis, we assume an ideal state, which neglects the effects of eddy currents and iron losses. The mathematical model of PMSM can be described by the following voltage equations in the dq synchronous rotating coordinate system:

$$\begin{cases} u_d = R_s i_d + \frac{d\psi_d}{dt} - \omega_e \psi_q \\ u_q = R_s i_q + \frac{d\psi_q}{dt} + \omega_e \psi_d \end{cases} \tag{1}$$

The solution to the flux linkage equations is as follows:

$$\begin{cases} \psi_d = L_d i_d + \psi_f \\ \psi_q = L_q i_q \end{cases} \tag{2}$$

where i_d, i_q, u_d, and u_q represent the dq-axis stator current and voltage, while R_s denotes the stator resistance. The ψ_d and ψ_q correspond to the dq-axis rotor flux linkage, while ω_e represents the electrical angular velocities of the rotor. The L_d and L_q represent the dq-axis inductance, and ψ_f denotes the permanent magnet rotor flux linkage.

Substituting Eq.(2) into Eq.(1) and adopting the $i_d{}^* = 0$ vector control method for decoupling control, we can obtain the following expressions for the stable state, where $di_d/dt = 0$ and $di_q/dt = 0$:

$$\begin{cases} u_d = R_s i_d - \omega_e L_q i_q \\ u_q = R_s i_q + \omega_e L_d i_d + \omega_e \psi_f \end{cases} \tag{3}$$

This paper focuses on parameter identification of surface-mounted PMSMs, where the dq-axis inductance can be assumed to be equal, i.e., $L_d = L_q = L_s$. To facilitate parameter identification, Eq. (3) needs to be transformed into a steady-state discrete equation. Since three motor parameters $\{R_s, L_s, \psi_f\}$ need to be solved for, Eq.(3) is an underdetermined system of rank 2, which cannot be solved uniquely on its own. To overcome this issue, this paper injects a negative-sequence weak magnetic current with $i_d{}^* \neq 0$ into the motor during steady-state operation, as shown in Fig. 1, to generate another set of second-order voltage equations. As a result, a full-rank equation system is obtained, with a unique solution. The final equation system for PMSM dq-axis identification is expressed as follows:

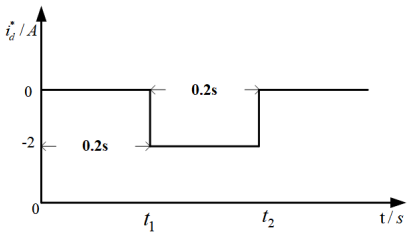

FIGURE 1. The waveform of the d-axis instantaneous negative-sequence current injection.

$$\begin{cases} u_{d0}(k) = -\hat{L}_s \omega_{e0}(k) i_{q0}(k) \\ u_{q0}(k) = \hat{R}_s i_{q0}(k) + \hat{\psi}_f \omega_{e0}(k) \\ u_d(k) = \hat{R}_s i_d(k) - \hat{L}_s \omega_e(k) i_q(k) \\ u_q(k) = \hat{R}_s i_q(k) + \hat{L}_s \omega_e(k) i_q(k) + \hat{\psi}_f \omega_e(k) \end{cases} \tag{4}$$

In the equation, $u_{d0}(k)$, $u_{q0}(k)$, $i_{d0}(k)$, $i_{q0}(k)$ represent the k-th sampling data of time period $i_d{}^* = 0$, while $u_d(k)$, $u_q(k)$, $i_d(k)$, $i_q(k)$ represent the k-th sampling data of time period $i_d{}^* = -2$, and $\{\hat{R}_s, \hat{L}_s, \hat{\psi}_f\}$ represent the identified motor parameter results of the algorithm.

III. ALGORITHM IMPROVEMENT

A. RAO-1 ALGORITHM

The RAO algorithms, proposed by Rao for unconstrained optimization problems [31], have great potential in the field of parameter identification and have already been applied in numerous industrial fields. The basic version of this algorithm is the RAO-1 algorithm. In comparison to RAO-2 and RAO-3 algorithms, the primary advantage that best characterizes the RAO algorithm is its simplicity in core formulas and fast iteration speed. It uses the optimal and worst solutions obtained during the iteration process to generate new solutions. The candidate solutions are updated using only two basic operations: addition and multiplication. Therefore, the RAO-1 algorithm has extremely low hardware requirements and is more easily implemented across platforms. The RAO-1 algorithm has only two simple parameters, namely the number of iterations and the population size. The core formula of RAO-1 is as follows:

$$X'_{j,h,i} = X_{j,h,i} + rand \cdot (X_{j,best,i} - X_{j,worst,i}) \tag{5}$$

where $X_{j,h,i}$ represents the solution vector of variable j in the h-th candidate solution at the i-th iteration; $X'_{j,h,i}$ is

the updated solution vector of $X_{j,h,i}$; $X_{j,best,i}$ represents the optimal solution vector of variable j in the h-th candidate solution at the i-th iteration; $X_{j,worst,i}$ represents the worst solution vector of variable j at the i-th iteration, and *rand* is a random variable between 0 and 1.

B. CGCRAO ALGORITHM DESIGN

1) INITIALIZATION OF TENT CHAOTIC MAPPING

Chaos has randomness, ergodicity, and initial value sensitivity, which can accelerate the convergence speed of the algorithm. In this paper, the Tent map is used to generate chaotic sequences, and the population is initialized to distribute the initial solutions as evenly as possible in the solution space. The process of generating a chaotic sequence Z based on the Tent map is as follows:

$$Z_h = \begin{cases} rand, & h = 1 \\ \frac{Z_{h-1}}{c}, & 0 \le Z_{h-1} < c \& 1 < h \\ \frac{1-Z_{h-1}}{1-c}, & c \le Z_{h-1} < 1 \& 1 < h \end{cases} \tag{6}$$

Here, c represents the chaos coefficient, which measures the complexity and disorder of the chaotic system. Z_h represents the h-th candidate solution in the initial population. In this paper, c is set to 0.5, which can generate a uniformly distributed sequence and make the initial population density insensitive to parameter changes. The initial population based on the Tent map chaotic mapping is illustrated as:

$$X_{j,h} = X_{j,min} + Z_h \cdot \left(X_{j,max} - X_{j,min}\right) \tag{7}$$

where $X_{j,h}$ represents the variable j in the h-th candidate solution in the initial population. $X_{j,min}$ and $X_{j,max}$ represent the upper and lower bounds of the candidate solution. Using an initial population based on the Tent chaotic mapping can improve the diversity of the population and to some extent improve the convergence speed.

2) MIXED VARIATION STRATEGY

The Gaussian distribution is a widely used probability distribution in mathematics, physics, and engineering. It has several characteristics: it can loosely explain several random variables and events in reality and can be used to estimate or extract several probability models. The probability density function of the Gaussian distribution is expressed as stated below:

$$f(x) = \frac{1}{\sqrt{2\pi}\sigma} \exp\left(-\frac{(x-\mu)^2}{2\sigma^2}\right) \tag{8}$$

where σ represents the variance and μ represents the mean. The operation of improving the local search performance of the key search area is called variation. Gaussian variation refers to the use of random numbers that conform to a normal distribution to guide the variation process. In previous studies, the grasshopper optimization algorithm, the moth-flame optimization algorithm, and the imperial competition optimization algorithm have all introduced Gaussian variation, which has enhanced the performance of their respective basic versions. When the algorithm enters the convergence state, the new solution update formula for Gaussian variation is as follows:

$$X'_{j,best,i} = X_{j,best,i} \cdot (1 + Gaussian(0, 1)) \tag{9}$$

The distribution of Gaussian variation is characterized by a mean of 1 and a variance of 0. When RAO-1 reaches convergence, the algorithm can explore new solutions in the vicinity of the optimal solution, which allows it to escape from local optima.

Cauchy distribution is a continuous probability distribution with an undefined mean. When a random variable x follows the probability density function of the Cauchy distribution, it is said to have a Cauchy distribution. The probability density function of the Cauchy distribution is given by:

$$f(x, \delta, \mu) = \frac{1}{\pi}\left(\frac{\delta}{\delta^2 + (x-\mu)^2}\right), -\infty < x < \infty \tag{10}$$

When we say a variable x follows the standard Cauchy distribution, it means that its probability density function is in the way described below:

$$f(x) = \frac{1}{\pi}\left(\frac{1}{x^2+1}\right), -\infty < x < \infty \tag{11}$$

To calculate the Cauchy distribution function, we can get by Eq.(11):

$$\text{Cauchy}(0, 1) = \tan\left(\left[\varepsilon - \frac{1}{2}\right]\pi\right), \varepsilon \in \text{U}(0, 1) \tag{12}$$

In this paper, Cauchy variation is used to update the best individual during algorithm convergence, which is highly effective in improving population diversity, escaping local optima, and enhancing the exploration properties of RAO-1. When the algorithm enters the convergence state, the Cauchy variation formula is as follows:

$$X'_{j,best,i} = X_{j,best,i} \cdot (1 + Cauchy(0, 1)) \tag{13}$$

To fully exploit the characteristics of the two various strategies mentioned above, the distribution of the Gaussian function and standard Cauchy function are compared in Fig. 2.

Through Fig. 2, it can be observed that the Gaussian distribution has a more centralized distribution compared to the standard Cauchy distribution, while the latter has more dispersed distribution on both sides. This indicates that the Cauchy distribution can generate a random number that is far away from the origin with a higher probability, making it more likely to escape from local optimal solutions and explore global optimal solutions. On the other hand, the Gaussian distribution can produce random numbers around the origin with a higher probability, which can enhance the exploration for better solutions around the current local optimal point, and thus accelerate the local search ability and speed of the RAO-1 algorithm. Therefore, this paper combines the advantages of both variation strategies and the Tent chaotic mapping to propose the CGCRAO algorithm.

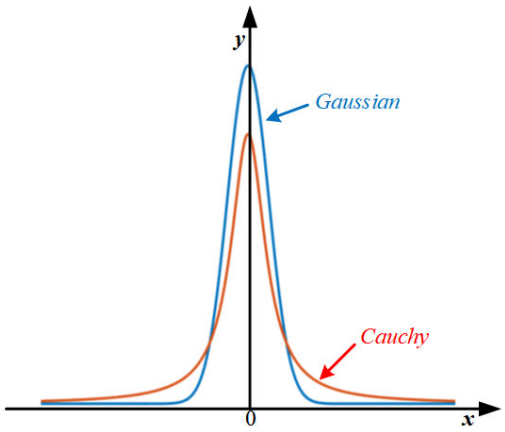

FIGURE 2. Gaussian Cauchy function comparison diagram.

3) CGCRAO ALGORITHM

When the chaotic RAO-1 algorithm reaches a relatively stable local optimal point, the Gaussian variation can be employed to focus on exploring the local area around the current optimal individual, thereby enhancing the algorithm's local search capability. Subsequently, when the Gaussian variation locates the optimal point within the current region, the Cauchy variation can be leveraged to increase the likelihood of the algorithm escaping from the local optimal point and improving its global exploration capability. To endow the proposed algorithm with the ability to autonomously select variation strategies, a three-stage operation idea is introduced to guide the variation process.

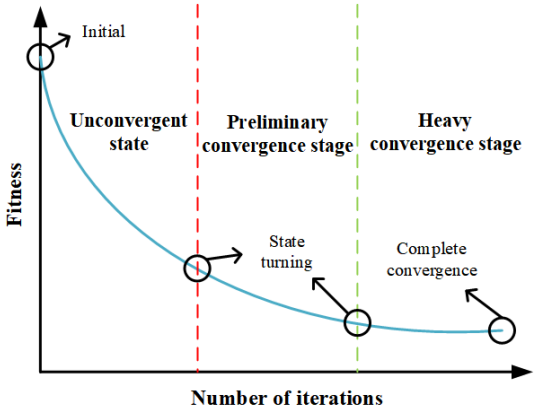

FIGURE 3. Algorithmic iterative process.

Drawing on the concept of slope in mathematics, the slope represents the degree of inclination of a straight line (or a tangent to a curve) with respect to the positive direction of the horizontal axis, reflecting the rate of change of the function value at that point. Its numerical value is the tangent of the angle between the horizontal axis and the line.

As shown in Fig. 3, the iterative operation of the algorithm is a process in which the adaptive function value continuously decreases and finally stabilizes at a minimum value, and the change in the function value approaches zero. Based on the analysis of the slope and the adaptive function, this paper analogizes the slope of the adaptive function curve using the difference in the adaptive function values of the best individuals in two iterations and provides two parameter values, k_1 and k_2. The algorithm is initialized, and when the total number of iterations reaches one-fifth, if the slope of the algorithm at this point is greater than k_1, it indicates that the algorithm is still in an unconverted state. If the slope is less than k_1 but greater than k_2, it indicates that the algorithm has entered the preliminary convergence state. When the slope of the algorithm is less than k_2, it indicates that the algorithm has entered the severe convergence state.

The selection of k_1 and k_2 impacts the global exploration ability and local exploitation ability of the CGCRAO algorithm. To determine the values of k_1 and k_2 for the CGCRAO algorithm in specific scenarios, it is necessary to analyze the convergence characteristics of the RAO-1 algorithm, which can include the average or standard deviation of fitness function values. In the context of PMSM parameter identification, this paper sets k_1 as the unit order of magnitude of the algorithm's average fitness function value and k_2 as one-tenth of k_1.

Different convergence states adopt different individual updating strategies. In the unconvergent state, the RAO-1 core formula Eq.(5) is used for iteration to drive the algorithm from the initial state toward the preliminary convergence state. After finding the local optimal point, the algorithm enters the second state - the preliminary convergence state, and uses the Gaussian variation core formula Eq.(9) for iteration to explore further the current local optimal point. Then, the algorithm enters the third phase - the heavy convergence state, and to improve the algorithm's global search capability, the Cauchy variation core formula Eq.(13) is selected for iteration to drive the algorithm from the severe convergence state toward the complete convergence state, attempting to escape the current local optimal point until the algorithm ends.

Through the above analysis, it is evident that the CGCRAO algorithm proposed in this paper introduces chaotic initialization and a Gaussian-Cauchy hybrid variation strategy, building upon the foundation of the RAO algorithm. Additionally, the CGCRAO algorithm is guided by the proposed three-stage concept to adapt its variation strategy based on the current search conditions, enhancing the algorithm's population diversity, global search, and local exploitation capabilities."

4) ALGORITHM PERFORMANCE TEST

In this section, the effectiveness of the proposed improved algorithm and the correctness of the three-stage idea are verified through 8 benchmark functions. The specific information of the functions is shown in Table 1. Among them, f_1, f_2, f_3, and f_4 are unimodal functions (with only one global optimum), which are used to test the algorithm's local exploitation capability. f_5, f_6, f_7, and f_8 are multimodal functions (real-valued functions with multiple local minima

TABLE 1. Information of eight benchmark functions.

Function	Formula	Parameter range	Optimum
Sphere	$f_1(x) = \sum_{i=1}^{D} x_i^2$	$[-100, 100]^D$	0
Rothyp	$f_2(x) = \sum_{i=1}^{D} \sum_{j=1}^{i} x_j^2$	$[-65.536, 65.536]^D$	0
Schwefel	$f_3(x) = \sum_{i=1}^{D} \lvert x_i \rvert + \prod_{i=1}^{D} \lvert x_i \rvert$	$[-30, 30]^D$	0
Sumsqu	$f_4(x) = \sum_{i=1}^{D} i x_i^2$	$[-10, 10]^D$	0
Zakharov	$f_5(x) = \sum_{i=1}^{D} x_i^2 + \left(\sum_{i=1}^{D} 0.5 i x_i\right)^2 + \left(\sum_{i=1}^{D} 0.5 i x_i\right)^4$	$[-5, 10]^D$	0
Rosenbrock	$f_6(x) = \sum_{i=1}^{D} [100(x_{2i-1}^2 - x_{2i})^2 + (x_{2i-1} - 1)^2]$	$[-100, 100]^D$	0
Quartic	$f_7(x) = \sum_{i=1}^{D} i x_i^4 + rand[0, 1)$	$[-1.28, 1.28]^D$	0
Griewank	$f_8(x) = \frac{1}{4000} \sum_{i=1}^{D} x_i^2 - \prod_{i=1}^{D} \cos(\frac{x_i}{\sqrt{i}}) + 1$	$[-600, 600]^D$	0

in the considered range), which are used to test the algorithm's global exploration capability.

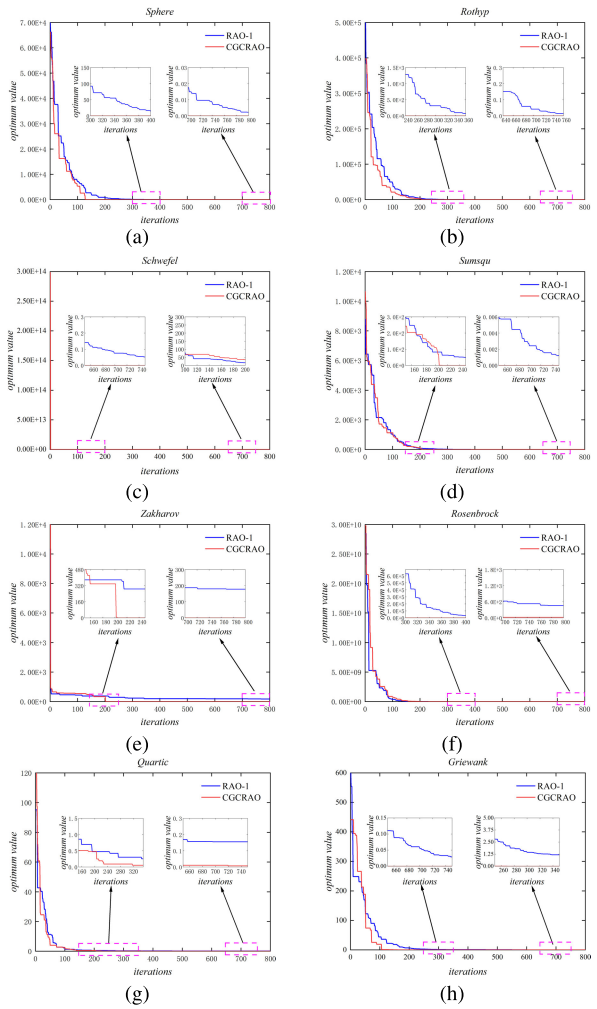

FIGURE 4. Comparison of convergence curves of eight benchmark test functions.

Fig. 4 presents a comparison of the results obtained by the CGCRAO and RAO-1 algorithms on eight benchmark functions. It can be observed that the CGCRAO exhibits a higher convergence rate and solution accuracy. Especially when dealing with multimodal functions like f_5, f_6, f_7, and f_8, the superior performance of CGCRAO is more pronounced. The chaotic initialization strategy enables the initial solution to be distributed as uniformly as possible in the solution space, while the Gaussian variation strengthens the algorithm's local exploration ability around the current best solution, and the Cauchy variation improves the algorithm's ability to jump out of local optima, providing stronger global exploration ability.

To further validate the correctness of dividing the algorithm into three stages, under the same control conditions with the introduction of Gaussian Cauchy variation and chaotic initialization, CGCRAO adopted the three-stage operation idea for autonomous selection of variation strategies, while CCGRAO used random numbers to select variation strategies. Table 2 presents a quantitative comparison of the two algorithms on 10 standard tests, each run 10 times (including mean and standard deviation values).

As shown in Table 2, CGCRAO using the three-stage running idea outperforms the mixed variation CCGRAO using random numbers in terms of both the best average value and standard deviation. This undoubtedly proves the correctness of dividing the algorithm into three stages, which endows the algorithm with autonomous selection ability. Compared with CCGRAO, CGCRAO exhibits stronger global optimization ability and more stable convergence accuracy.

IV. PMSM PARAMETER IDENTIFICATION BASED ON CGCRAO

A. PRINCIPLE OF PMSM PARAMETER IDENTIFICATION

The basic principle of PMSM parameter identification is to continuously refine the adaptive function value of the

TABLE 2. Comparative experimental results of ideological verification.

Function	Descriptive analysis	CGCRAO	CCGRAO
Sphere	Mean	8.9004e-143	2.9950e-13
	Std	2.9519e-142	7.2771e-13
Rothyp	Mean	5.2820e-140	6.5046e-11
	Std	1.7375e-139	1.7728e-10
Schwefel	Mean	5.8252e-73	5.6568e-06
	Std	1.7867e-72	1.7848e-05
Sumsqu	Mean	4.5484e-141	1.3130e-11
	Std	1.5085e-140	4.3159e-11
Zakharov	Mean	2.8204e-154	4.0828e-15
	Std	8.9187e-154	1.1350e-14
Rosenbrock	Mean	24.8381	25.4177
	Std	0.2400	0.2857
Quartic	Mean	0.0031	0.0220
	Std	0.0025	0.0285
Griewank	Mean	0	5.7579e-09
	Std	0	1.8173e-08

identification parameters through optimization algorithms based on the difference between the electric machine theoretical model and the actual system output, and ultimately converge to the parameter values with the minimum fitness, thus obtaining the PMSM parameters. The PMSM parameter identification model is shown in Fig. 5.

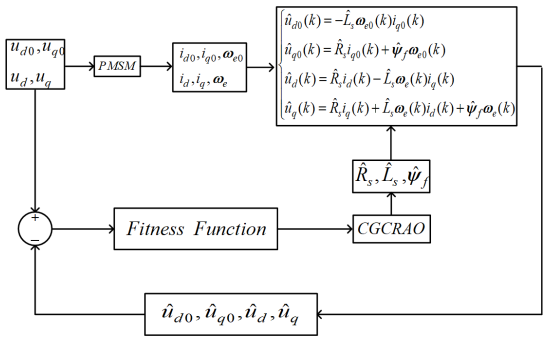

FIGURE 5. PMSM parameter identification model.

The Fitness function in Fig. 5 is as follows:

$$\begin{aligned} Fitness =& \omega_1 \cdot \left|u_{d0}(k) - \hat{u_{d0}}(k)\right| \\ &+ \omega_2 \cdot \left|u_d(k) - \hat{u_d}(k)\right| \\ &+ \omega_3 \cdot \left|u_{q0}(k) - \hat{u_{q0}}(k)\right| \\ &+ \omega_4 \cdot \left|u_q(k) - \hat{u_q}(k)\right| \end{aligned} \tag{14}$$

In the above equation, ω_1, ω_2, ω_3, and ω_4 are the weighting coefficients of the Fitness function. When the fitness value is the same, different weighting coefficients will lead to different accuracy of the identification results. u_{d0} and u_{q0} represent the measured values of the motor dq-axis voltage under $i_d{}^* = 0$ control, while $\hat{u_{d0}}$ and $\hat{u_{q0}}$ represent the corresponding estimated values obtained by the algorithm from the collected data under $i_d{}^* = 0$ control. u_d and u_q represent the motor dq-axis voltage measurement values obtained when injecting negative sequence current $i_d{}^*$ is not equal to 0, while $\hat{u_d}$ and $\hat{u_q}$ represent the corresponding estimated values obtained by the algorithm from the collected data when injecting negative sequence current $i_d{}^*$ is not equal to 0.

B. CGCRAO-BASED PMSM PARAMETER IDENTIFICATION STEPS

Step 1: Start running the PMSM and save the data for the motor operation in different $i_d{}^*$ modes, including dq-axis voltage, current, and electrical angular velocity.

Step 2: Set the population size and iteration times, and initialize the population using Tent chaotic mapping according to Eq.(6) and Eq.(7).

Step 3: Determine whether the maximum number of iterations has been reached. If "yes," then execute Step 8. If "no," then execute Steps 4 to 7.

Step 4: Calculate the individual's fitness function value using Eq.(4) and Eq.(14). Find the best and worst value individuals and their corresponding fitness function values.

Step 5: Update the individual according to the convergence state. If the convergence state is not reached, use the RAO-1 core formula Eq.(5) for individual updating. If the convergence state is reached preliminarily, use the Gaussian variation core formula Eq.(9) for individual updating. If the convergence state is reached heavily, use the Cauchy variation core formula Eq.(13) for individual updating.

Step 6: Handle the boundary and calculate the fitness function value of the new individual.

Step 7: Determine whether the new individual is better than the old individual. If "yes," then replace the old individual with the new one. If "no," then keep the old individual. Then execute Steps 3.

Step 8: Output the best individual and its corresponding fitness function value. The optimal individual $\{\hat{R}_s, \hat{L}_s, \hat{\psi}_f\}$ is the result of identifying the motor parameters, which continues until the algorithm ends.

Fig. 6 depicts the process flowchart of the CGCRAO algorithm for PMSM parameter identification.

V. SIMULATION VERIFICATION

An SVPMSM identification system was built on the Matlab/Simulink software platform to validate the effectiveness and feasibility of the proposed CGCRAO-based algorithm for PMSM parameter identification. It is shown in Fig. 7. The motor utilizes a vector control strategy, and the algorithm's input signals consist of u_d, u_q, i_d, i_q, and ω_e. Table 3 displays the specific parameters of the SVPMSM utilized in the experiment.

The total simulation time is 0.4 seconds. Table 4 presents the algorithm's parameter settings, where W represents the inertia weight, C_1 represents the self-learning factor, C_2 represents the social learning factor, pop represents the population size, N represents the total number of iterations, Cr represents the crossover rate, F represents the scaling factor, and k_1, k_2 represent the various factors in CGCRAO.

1) Operating condition 1.

The identification results and errors under a no-load condition at a speed of 1000 rpm are presented in Table 5. Fig. 8 illustrates the fitness functions and parameter identification curves for five algorithms applied to PMSM parameter identification.

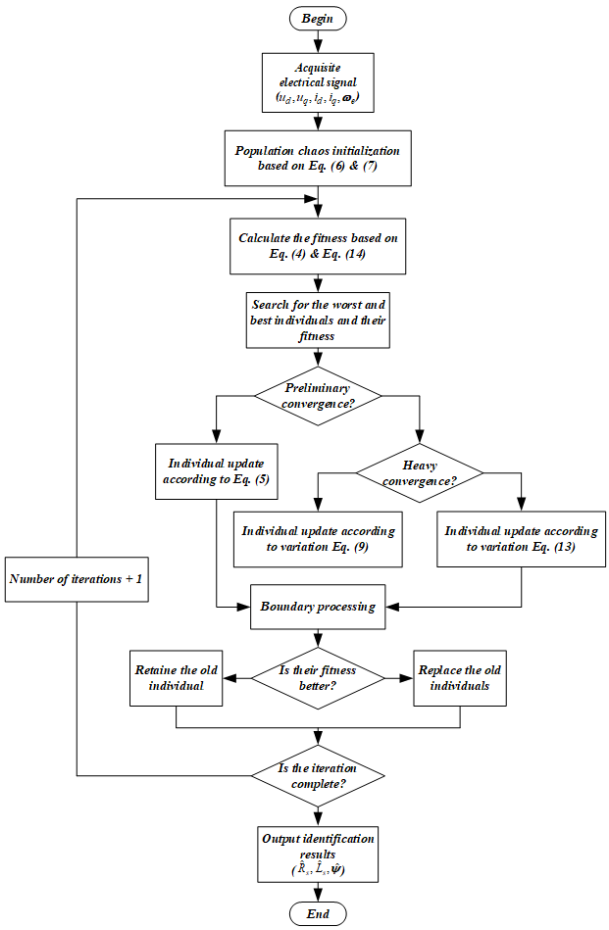

FIGURE 6. The process flowchart for PMSM parameter identification base on CGCRAO algorithm.

TABLE 3. Specific motor parameters.

Parameter of electric machine	Value
Number of pole pairs Pn	4
Stator resistance R_s	12.8 Ω
Stator inductance L_d	30.2 mH
Flux linkage ϕ_f	0.204 Wb
Inertia	0.00017 kg·m^2
Rated torque	0.637 N·m/A
Bus voltage	400 V
Switching frequency	10 kHz

TABLE 4. Parameter settings for the five algorithms.

Algorithm	Parameter Settings
PSO	$W = 0.8; C_1 = C_2 = 1.4; pop = 100; N = 200;$
DE	$C_r = 0.9; F = 0.5; pop = 100; N = 200;$
GWO	$pop = 100; N = 200;$
RAO-1	$pop = 100; N = 200;$
CGCRAO	$k_1 = 0.8; k_2 = 0.01; pop = 100; N = 200;$

The identification results of a dual closed-loop vector-controlled PMSM under Operating condition 1, obtained by running simulations and comparing five intelligent algorithms, reveal that The DE, PSO, RAO-1, GWO, and CGCRAO algorithms converge to stability after 19, 10, 25, 60, and 47 iterations, respectively. The final fitness values of the five algorithms are 0.03845, 0.03682, 0.02935, 0.02661, and 0.02411, respectively. The RAO-1, DE, and PSO algorithms are more prone to local optima. Compared to the DE and PSO algorithms, the RAO-1 algorithm not only achieves higher identification accuracy and similar convergence speed but also has a relatively simple core formula, making it more suitable for PMSM parameter identification. In contrast, although GWO surpasses RAO-1 in terms of identification accuracy, it exhibits slower convergence speed and requires further improvement. The proposed CGCRAO algorithm, which incorporates a hybrid variation and chaotic initialization strategy, outperforms other algorithms in terms of convergence speed and accuracy. The identification results of stator resistance, stator inductance, and magnetic flux shown in Fig. 8 demonstrate that the CGCRAO algorithm converges to the true values faster and more smoothly. Finally, when considering Table 5, it is evident that the identification errors of various parameters in CGCRAO are significantly smaller than those in the other four algorithms. CGCRAO inherits the fast convergence property of RAO-1 while achieving higher identification accuracy.

2) Operating condition 2.

The identification results and errors under a speed of 1500 rpm and rated torque are presented in Table 6. The fitness function curve and parameter identification variation curves are shown in Fig. 9.

Even with increased motor speed and torque, the CGCRAO algorithm maintains identification errors of less than 1% for resistance and magnetic flux, with an identification error of only 1.0547% for inductance. Although both GWO and RAO-1 algorithms have identification errors within 2%, the GWO algorithm exhibits the slowest identification speed and significant parameter fluctuation. Both PSO and DE algorithms have resistance identification errors exceeding 4.5%, indicating poor identification performance and practicality. It is evident from the fitness function curve that the CGCRAO algorithm maintains the highest identification accuracy and a very fast convergence speed. From Fig. 9, it can be observed that the parameter identification curves of the CGCRAO algorithm exhibit minimal fluctuation, indicating good robustness under different operating conditions.

VI. EXPERIMENTAL VERIFICATION

To further validate the feasibility and correctness of the proposed CGCRAO algorithm for PMSM parameter identification. The hardware experimental platform, as shown in Fig. 10, was constructed, consisting of a 0.2 kW PMSM, motor driver, microcontroller, host computer, isolation transformer, and oscilloscope. The floating-point DSP TMS320F28335 controller from TI Corporation was used in this paper. The design of the motor vector control algorithm was completed in the Code Composer Studio software. The system control program consists of a main program and a loop timer interrupt program. The interrupt function completes tasks such as A/D sampling, position and velocity

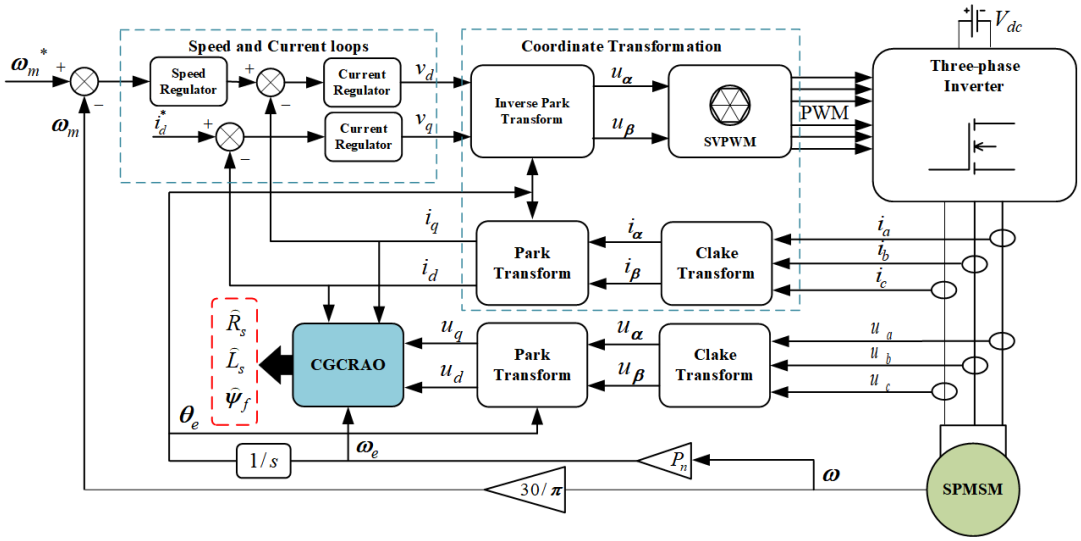

FIGURE 7. The framework of PMSM identification based on CGCRAO algorithm.

TABLE 5. Parameter identification results by using five algorithms under Operating condition 1 in the simulation environment.

Parameter	True value	Descriptive statistics	DE	PSO	RAO-1	GWO	CGCRAO
R_s/Ω	12.8	Identification value	13.5347	12.1909	13.0469	12.5922	12.6861
		Error(%)	5.7396	4.7585	1.9293	1.6234	0.8901
L_s/mH	30.2	Identification value	29.4677	30.9983	29.8337	30.5314	30.4589
		Error(%)	2.4247	2.6433	1.2129	1.0975	0.8572
ϕ_f/Wb	0.08833	Identification value	0.0861	0.0899	0.0876	0.0891	0.0888
		Error(%)	2.4728	1.7343	0.8581	0.8287	0.4827

TABLE 6. Parameter identification results by using five algorithms under Operating condition 2 in the simulation environment.

Parameter	True value	Descriptive statistics	DE	PSO	RAO-1	GWO	CGCRAO
R_s/Ω	12.8	Identification value	13.4947	13.4304	13.0504	12.6213	12.6729
		Error(%)	5.4270	4.9250	1.9544	1.3960	0.9929
L_s/mH	30.2	Identification value	29.4507	29.5404	30.5756	30.5767	30.5185
		Error(%)	2.4810	2.1840	1.2436	1.2472	1.0547
ϕ_f/Wb	0.08833	Identification value	0.0901	0.0900	0.0876	0.0891	0.0890
		Error(%)	2.0058	1.8369	0.8582	0.8821	0.8143

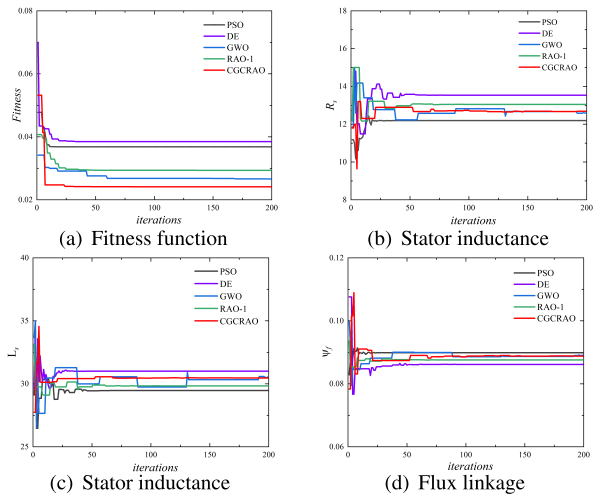

(a) Fitness function (b) Stator inductance (c) Stator inductance (d) Flux linkage

FIGURE 8. Parameter identification curves of PMSM using five algorithms under Operating condition 1 in the simulation environment.

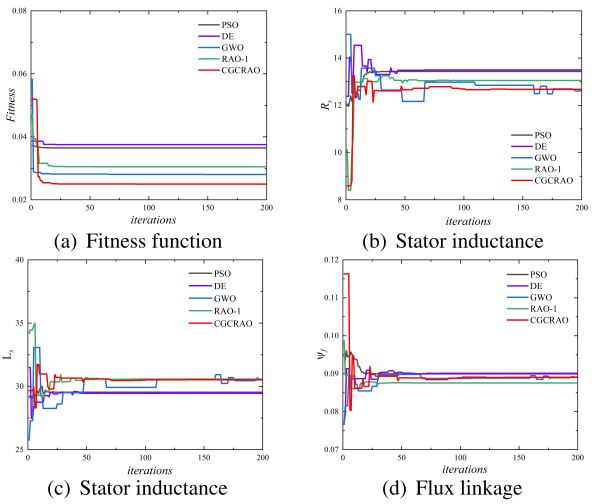

(a) Fitness function (b) Stator inductance (c) Stator inductance (d) Flux linkage

FIGURE 9. Parameter identification curves of PMSM using five algorithms under Operating condition 2 in the simulation environment.

estimation, coordinate transformation, velocity and current PI control, and SVPWM modulation within the timer period. The real-time communication between the microcontroller and the host computer is used to obtain the current, voltage,

and rotational speed information required for algorithm identification.

The experiment validation includes motor parameter identification experiments under two different operating conditions and algorithm identification time testing.

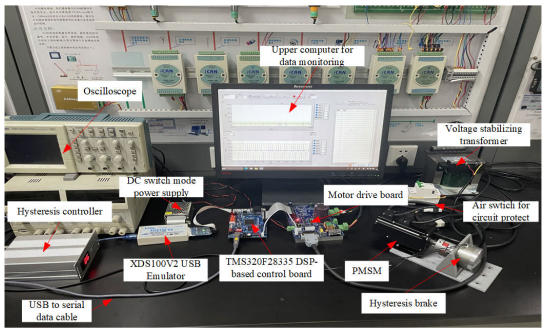

FIGURE 10. Experimental platform.

1) Operating condition 1.

The identification results and errors at the unloaded state with a rotational speed of 1000 rpm are shown in Table 7. The adaptive function curve and the curves depicting parameter identification variations are shown in Fig. 11.

By observing the adaptive fitness function curves of the five functions in Fig. 11, it can be seen that CGCRAO converges to the lowest fitness value, which is 0.03306. The final fitness values for parameter identification using GWO and RAO-1 are close, but RAO-1 demonstrates greater stability and faster convergence compared to GWO. The CGCRAO algorithm is based on simplicity and fewer parameters of the core formula of RAO-1, and it also exhibits a similarly fast convergence speed. PSO and DE algorithms have the lowest parameter identification accuracy, with final fitness values of 0.4002 and 0.04113, respectively.

The identification error of motor resistance under the same operating condition is relatively higher compared to the simulation results, which is mainly attributed to sensor accuracy and external environmental interference on the motor. Among different algorithms used for the identification of stator resistance, electronic inductance, and magnetic flux parameters, CGCRAO achieves the highest accuracy with identification errors of 2.5898%, 1.7506%, 0.5907%, and it also exhibits fast convergence speed. In comparison, the RAO-1 algorithm exhibits the fastest convergence speed but is prone to getting trapped in local optima, leading to improved accuracy. The major issue with the GWO algorithm is its unstable identification results with the highest fluctuation. PSO and DE algorithms provide relatively close identification results to the actual value for inductance, but they perform the worst in terms of resistance and magnetic flux identification.

2) Operating condition 2.

The parameter identification of the five algorithms was conducted under the operating condition of the motor with a speed of 1500 rpm and rated torque. The identification

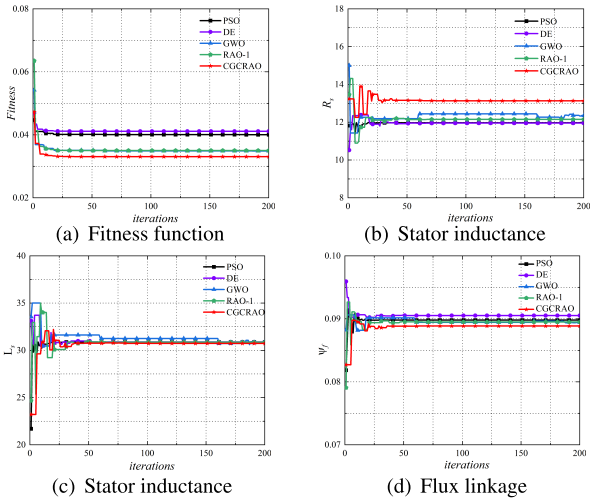

FIGURE 11. Parameter identification curves of PMSM using five algorithms under Operating Condition 1 in the physical motor environment.

curves and fitness function curves are depicted in Fig. 12. The identification results and errors are listed in Table 8.

Operating condition 2 imposes stricter requirements on the motor's speed and load, primarily testing the robustness and stability of different algorithms under complex conditions. From the graph, it can be observed that the DE algorithm exhibits the largest variations, the highest fitness value, and the poorest accuracy. The CGCRAO algorithm shows smaller variations and remains the most accurate among the five algorithms, demonstrating good robustness and stability for motor parameter identification under different operating conditions. Increasing torque and speed lead to larger identification errors, with the most significant changes observed in resistance and magnetic flux. Although the GWO algorithm demonstrates decent convergence accuracy, it exhibits greater fluctuations in parameter identification under operating condition 2. In comparison, RAO-1 and CGCRAO exhibit better practicality in motor parameter identification. The CGCRAO algorithm, when combined with chaotic initialization and a Gaussian-Cauchy hybrid mutation strategy, exhibits improved identification accuracy and stability compared to the RAO-1 algorithm.

3) Execution Time Test for Algorithm Parameter.

Identification Perform 10 runs for each of the aforementioned two operating conditions and calculate the average execution time for the five algorithms. To compare the computational workload of the five algorithms, this study employed a combination of the pre-estimate method and the post-statistical method. Factors such as algorithm population size, iteration times, core formula, programming language, and machine execution speed were considered. The algorithm's execution time (averaged over 20 runs) was used to reflect its computational workload under the condition of maintaining the consistency of these factors. This is illustrated in Table 9.

TABLE 7. Parameter identification results by using five algorithms under Operating condition 1 in the physical motor environment.

Parameter	True value	Descriptive statistics	DE	PSO	RAO-1	GWO	CGCRAO
R_s/Ω	12.8	Identification value	11.9502	11.9702	12.1466	12.3503	13.1315
		Error(%)	6.6392	6.4832	5.1044	3.5133	2.5898
L_s/mH	30.2	Identification value	30.8857	30.8890	30.8617	30.8179	30.7287
		Error(%)	2.2707	2.2815	1.1910	1.0460	1.7506
ϕ_f/Wb	0.08833	Identification value	0.0905	0.0898	0.0895	0.0894	0.0889
		Error(%)	2.4693	1.6556	1.3122	1.2228	0.5907

TABLE 8. Parameter identification results by using five algorithms under Operating condition 2 in the physical motor environment.

Parameter	True value	Descriptive statistics	DE	PSO	RAO-1	GWO	CGCRAO
R_s/Ω	12.8	Identification value	13.4368	13.3059	12.3447	12.3937	13.2053
		Error(%)	4.9754	3.9525	3.5573	3.1746	3.1662
L_s/mH	30.2	Identification value	30.9568	30.9350	30.8415	30.8525	30.7454
		Error(%)	2.5061	2.4338	2.1242	2.1606	0.8060
ϕ_f/Wb	0.08833	Identification value	0.0902	0.0901	0.0900	0.0897	0.0889
		Error(%)	2.0738	2.0011	1.8990	1.5997	0.6401

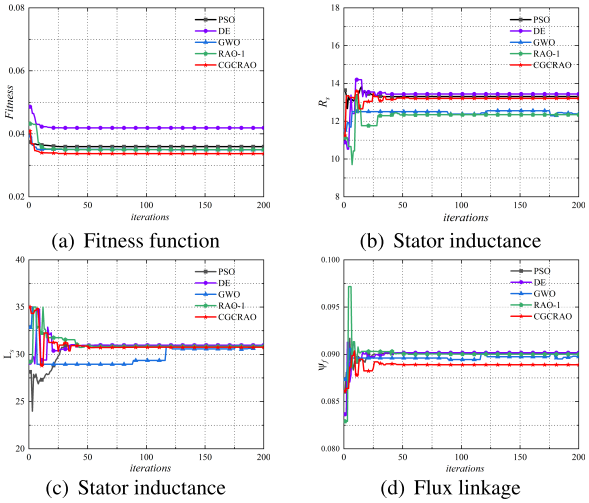

(a) Fitness function (b) Stator inductance

(c) Stator inductance (d) Flux linkage

FIGURE 12. Parameter identification curves of PMSM using five algorithms under Operating Condition 2 in the physical motor environment.

TABLE 9. Comparison of five algorithms execution time.

Algorithm	Running time
DE	0.6503 s
PSO	0.5563 s
RAO-1	0.4795 s
GWO	0.5717 s
CGCRAO	0.5043 s

We compared the running time of the five algorithms using a population size of 100 and 200 iterations. Table 9 shows that RAO-1 and CGCRAO algorithms have significantly shorter running time compared to DE, PSO, and GWO algorithms. This is due to the higher time complexity of DE, PSO, and GWO algorithms compared to RAO-1 and CGCRAO algorithms, resulting in longer running time and slower convergence. Despite introducing the Gaussian-Cauchy variation strategy and chaotic initialization strategy based on RAO-1, and selecting variation strategy according to different operating states, the CGCRAO algorithm maintains a fast running speed, as shown in the Table 9, even though these additions increase the computational complexity of the algorithm.

CGCRAO combines the advantages of the original RAO-1 algorithm, requiring fewer algorithm parameters and featuring a more concise core formula, resulting in high accuracy. Furthermore, CGCRAO demonstrates a wider applicability, making it suitable for identifying various types of motors including asynchronous motors and wind turbines.

VII. CONCLUSION

This paper proposes a hybrid variation-based chaotic RAO algorithm for PMSM parameter identification. The introduction of Tent chaotic mapping in the initialization stage enriches the population diversity and accelerates population convergence. Meanwhile, a three-stage operation idea is proposed to guide the Gaussian-Cauchy hybrid variation process. The effectiveness of the algorithm improvement and the correctness of the three-stage idea are verified through eight benchmark test functions. The simulations and experiments under various operating conditions indicate that the CGCRAO algorithm can identify the electromagnetic parameters of PMSM, such as stator resistance, inductance, and flux linkage. Compared with the identification results of PSO, DE, GWO, and the original version of the RAO-1 algorithm, CGCRAO exhibits fast convergence speed, high accuracy, and strong robustness. With fewer parameter settings and a core formula of addition and multiplication operations, the CGCRAO algorithm provides a new method for applying intelligent algorithms to embedded system applications for motor parameter identification.

REFERENCES

[1] J. Xu, S. Guo, H. Guo, and X. Tian, "Fault-tolerant current control of six-phase permanent magnet motor with multifrequency quasi-proportional-resonant control and feedforward compensation for aerospace drives," *IEEE Trans. Power Electron.*, vol. 38, no. 1, pp. 283–293, Jan. 2023.

[2] L. Tian, Z. Wang, Q. Yu, C. Tang, and H. Zhang, "Current reconstruction by one-step compensation for permanent magnet synchronous motor with fixed sampling interval in position sensorless control," *IEEE Trans. Ind. Electron.*, vol. 70, no. 1, pp. 200–210, Jan. 2023.

[3] Y. Tang, F. Chai, and L. Chen, "Investigation of open-circuit fault-tolerant strategy in a modular permanent magnet synchronous in-wheel motor based on electromagnetic–thermal analysis," *IEEE Trans. Transport. Electrific.*, vol. 8, no. 1, pp. 1085–1093, Mar. 2022.
[4] X. Fang, S. Lin, X. Wang, Z. Yang, F. Lin, and Z. Tian, "Model predictive current control of traction permanent magnet synchronous motors in six-step operation for railway application," *IEEE Trans. Ind. Electron.*, vol. 69, no. 9, pp. 8751–8759, Sep. 2022.
[5] R. Pothuraju, R. Tejavathu, and A. K. Panda, "Multilevel inverter fed direct torque and flux control-space vector modulation of speed sensorless permanent magnet synchronous motor drive with improved steady state and dynamic characteristics," *Int. J. Circuit Theory Appl.*, vol. 50, no. 4, pp. 1279–1296, Apr. 2022.
[6] D. M. Reed, J. Sun, and H. F. Hofmann, "Simultaneous identification and adaptive torque control of permanent magnet synchronous machines," *IEEE Trans. Control Syst. Technol.*, vol. 25, no. 4, pp. 1372–1383, Jul. 2017.
[7] C. Ma, J. Li, N. Zhang, F. Bu, and Z. Yang, "Open-circuit radial stray magnetic flux density based noninvasive diagnosis for mixed eccentricity parameters of interior permanent magnet synchronous motors in electric vehicles," *IEEE Trans. Ind. Electron.*, vol. 70, no. 2, pp. 1983–1992, Feb. 2023.
[8] C. Candelo-Zuluaga, J.-R. Riba, and A. Garcia, "PMSM parameter estimation for sensorless FOC based on differential power factor," *IEEE Trans. Instrum. Meas.*, vol. 70, pp. 1–12, 2021.
[9] C. Yang, L. Bu, and B. Chen, "Energy modeling and online parameter identification for permanent magnet synchronous motor driven belt conveyors," *Measurement*, vol. 178, Jun. 2021, Art. no. 109342.
[10] H. Yu, J. Wang, and Z. Xin, "Model predictive control for PMSM based on discrete space vector modulation with RLS parameter identification," *Energies*, vol. 15, no. 11, p. 4041, May 2022.
[11] X. Huang, Y. Yu, Z. Li, Z. Chen, S. Huang, F. Niu, and J. Zhang, "Online identification of inductance and flux linkage for inverter-fed SPMSMs using switching state functions," *IEEE Trans. Power Electron.*, vol. 38, no. 1, pp. 917–930, Jan. 2023.
[12] S. Wang, "Windowed least square algorithm based PMSM parameters estimation," *Math. Problems Eng.*, vol. 2013, pp. 1–11, Jan. 2013.
[13] T. Boileau, N. Leboeuf, B. Nahid-Mobarakeh, and F. Meibody-Tabar, "Online identification of PMSM parameters: Parameter identifiability and estimator comparative study," *IEEE Trans. Ind. Appl.*, vol. 47, no. 4, pp. 1944–1957, Jul. 2011.
[14] O. C. Kivanc and S. B. Ozturk, "Sensorless PMSM drive based on stator feedforward voltage estimation improved with MRAS multiparameter estimation," *IEEE/ASME Trans. Mechatronics*, vol. 23, no. 3, pp. 1326–1337, Jun. 2018.
[15] X. Zhang and Z. Li, "Sliding-mode observer-based mechanical parameter estimation for permanent magnet synchronous motor," *IEEE Trans. Power Electron.*, vol. 31, no. 8, pp. 5732–5745, Aug. 2016.
[16] G. Pei, J. Liu, L. Li, P. Du, L. Pei, and Y. Hu, "MRAS based online parameter identification for PMSM considering VSI nonlinearity," in *Proc. IEEE Int. Power Electron. Appl. Conf. Expo. (PEAC)*, Nov. 2018, pp. 1–7.
[17] Y. Shi, K. Sun, L. Huang, and Y. Li, "Online identification of permanent magnet flux based on extended Kalman filter for IPMSM drive with position sensorless control," *IEEE Trans. Ind. Electron.*, vol. 59, no. 11, pp. 4169–4178, Nov. 2012.
[18] H. Lin, H. Yan, Y. Ling, and M. Yan, "Design of dual extended Kalman filter for permanent magnet synchronous motor," in *Proc. 32nd Chin. Control Conf.*, Jul. 2013, pp. 1729–1734.
[19] X. Li and R. Kennel, "General formulation of Kalman-filter-based online parameter identification methods for VSI-fed PMSM," *IEEE Trans. Ind. Electron.*, vol. 68, no. 4, pp. 2856–2864, Apr. 2021.
[20] M. A. Ahandani, J. Abbasfam, and H. Kharrati, "Parameter identification of permanent magnet synchronous motors using quasi-opposition-based particle swarm optimization and hybrid chaotic particle swarm optimization algorithms," *Int. J. Speech Technol.*, vol. 52, no. 11, pp. 13082–13096, Sep. 2022.
[21] Z. Wang, M. Yang, L. Gao, Z. Wang, G. Zhang, H. Wang, and X. Gu, "Deadbeat predictive current control of permanent magnet synchronous motor based on variable step-size adaline neural network parameter identification," *IET Electr. Power Appl.*, vol. 14, no. 11, pp. 2007–2015, Nov. 2020.
[22] Z.-H. Liu, H.-L. Wei, X.-H. Li, K. Liu, and Q.-C. Zhong, "Global identification of electrical and mechanical parameters in PMSM drive based on dynamic self-learning PSO," *IEEE Trans. Power Electron.*, vol. 33, no. 12, pp. 10858–10871, Dec. 2018.
[23] X. Fu, H. Gu, and G. Chen, "Permanent magnet synchronous motors parameters identification based on Cauchy mutation particle swarm optimization," *Trans. China Electrotech. Soc.*, vol. 29, no. 5, pp. 127–131, 2014.
[24] Z.-H. Liu, H.-L. Wei, Q.-C. Zhong, K. Liu, X.-S. Xiao, and L.-H. Wu, "Parameter estimation for VSI-fed PMSM based on a dynamic PSO with learning strategies," *IEEE Trans. Power Electron.*, vol. 32, no. 4, pp. 3154–3165, Apr. 2017.
[25] X. Ke, J. Zhang, W. Jian, G. Peng, and Y. Chen, "Multi-parameter identification of PMSM based on IGWO algorithm," in *Proc. Int. Workshop Adv. Manuf. Autom.* Cham, Switzerland: Springer, 2021, pp. 547–555.
[26] K. Lam, G. Feng, and Y. Han, "Identification of PMSM parameters based on differential evolution algorithm with multiple evolutionary strategies," in *Proc. China Autom. Congr. (CAC)*, Oct. 2021, pp. 4797–4802.
[27] H. Yang, J. Li, B. Liu, and L. Chen, "Identification of source information for sudden hazardous chemical leakage accidents in surface water on the basis of particle swarm optimisation, differential evolution and metropolis–hastings sampling," *Environ. Sci. Pollut. Res.*, vol. 28, pp. 67292–67309, Dec. 2021.
[28] S. Patel, T. I. Eldho, and A. K. Rastogi, "Hybrid-metaheuristics based inverse groundwater modelling to estimate hydraulic conductivity in a nonlinear real-field large aquifer system," *Water Resour. Manage.*, vol. 34, no. 6, pp. 2011–2028, Apr. 2020.
[29] B. Pourasghar, M. A. Ahandani, and H. Kharrati, "Parameter identification of engineering problems using a differential shuffled complex evolution," *Artif. Intell. Rev.*, vol. 53, no. 4, pp. 2749–2782, Apr. 2020.
[30] C. Wang, Y. Liu, X. Liang, H. Guo, Y. Chen, and Y. Zhao, "Self-adaptive differential evolution algorithm with hybrid mutation operator for parameters identification of PMSM," *Soft Comput.*, vol. 22, no. 4, pp. 1263–1285, Feb. 2018.
[31] R. V. Rao, "Rao algorithms: Three metaphor-less simple algorithms for solving optimization problems," *Int. J. Ind. Eng. Comput.*, vol. 11, no. 1, pp. 107–130, 2020.

HONGJI LI was born in Hengyang, Hunan, China, in 1999. He received the bachelor's degree in electronic information from Northeast Electric Power University, in 2021. He is currently pursuing the master's degree in information and communication engineering with the University of Shanghai for Science and Technology.

His research interests include machine learning, parameter identification of permanent magnet synchronous motors, and sensorless control strategies.

XIANZHONG JIAN was born in Shaoyang, Hunan, China, in 1969. He received the Ph.D. degree from the Chinese Academy of Sciences, in 2003.

He is currently a Professor with the School of Optoelectronic Information and Computer Engineering, University of Shanghai for Science and Technology. His research interests include embedded system design, applications of intelligent algorithms, infrared image processing, and motor drive technologies.